

JUN 12 1957

~~CONFIDENTIAL~~

Copy 4
RM E57D19

NACA RM E57D19



c1

RESEARCH MEMORANDUM

CASCADE INVESTIGATION OF COOLING CHARACTERISTICS OF A

CAST-FINNED AIR-COOLED TURBINE BLADE

FOR USE IN A TURBOPROP ENGINE

By Francis S. Stepka, Hadley T. Richards, and Robert O. Hickel

Lewis Flight Propulsion Laboratory
Cleveland, Ohio

CLASSIFICATION CHANGED

LIBRARY COPY

JUN 20 1957

To **UNCLASSIFIED**

LANGLEY AERONAUTICAL LABORATORY
LIBRARY, NACA
LANGLEY FIELD, VIRGINIA

By authority of *NASA ltr Dec 3, 1962*

dtd Nov. 14, 1962
s/Boyd C. Myers II

This material contains information affecting the National Defense of the United States within the meaning of the espionage laws, Title 18, U.S.C., Secs. 793 and 794, the transmission or revelation of which in any manner to an unauthorized person is prohibited by law.

Effective date:
July 17, 1962.

**NATIONAL ADVISORY COMMITTEE
FOR AERONAUTICS**

WASHINGTON

June 12, 1957

~~CONFIDENTIAL~~



NATIONAL ADVISORY COMMITTEE FOR AERONAUTICS

RESEARCH MEMORANDUMCASCADE INVESTIGATION OF COOLING CHARACTERISTICS OF A CAST-FINNED
AIR-COOLED TURBINE BLADE FOR USE IN A TURBOPROP ENGINE

By Francis S. Stepka, Hadley T. Richards, and Robert O. Hickel

SUMMARY

The cooling characteristics of a small air-cooled turbine blade for use in a turboprop engine were experimentally investigated in a static cascade facility. Three test blades of 1.4-inch span and 0.7-inch chord were studied at combustion-gas temperatures of about 1060°, 1360°, and 1660° R. The blade cooling-air temperatures ranged from about 580° to 1060° R. The gas Reynolds number was varied from about 70,000 to 170,000, a range comparable to that which might exist in a turboprop engine.

On the basis of a nondimensional method of correlating blade metal temperatures with combustion-gas and cooling-air conditions presented herein, average blade metal temperatures at particular span locations, local metal temperatures, and the average metal temperatures of the entire blade correlate within about 7 percent of a mean line drawn through the test data. The correlated data are applied to a typical turboprop engine in an attempt to obtain an insight into the probable cooling characteristics of the blade configuration under engine operating conditions at a turbine-inlet gas temperature of 2460° R. The analysis indicates that cooling-air requirements are about the same for both sea-level static conditions and for flight at 300 knots at a 30,000-foot altitude.

At 30,000 feet the ratio of cooling-air to combustion-gas flow necessary to maintain an average blade temperature of 1985° R is about 0.015. This value results in a blade stress-ratio factor (ratio of allowable stress-rupture strength for blade material to calculated average centrifugal stress at critical span location) of about 3, based on 1000-hour life. Past experience with much larger air-cooled blades, such as those used in turbojet engines, shows that stress-ratio factors on the order of 1.2 to 1.5 are required to obtain the desired blade life. Therefore, the finned-blade investigated appears to have a conservative (large) value of stress-ratio factor and a reasonable potentiality for satisfactory high-temperature engine operation at low coolant flow.

INTRODUCTION

The benefits that can be obtained by increasing the turbine-inlet temperature of turboprop engines and the thermodynamic effects of cooling the turbines on engine performance have been established and are reported in references 1 to 4. Because of the smallness of the turbine blades (generally blade chords less than 1 in. and blade spans of the order of 1 to 2 in.) in present-day turboprop engines, cooling and fabrication problems are likely to be more acute than those of larger-sized turbine blades such as are used in turbojet engines.

An analysis of the effect of turbine blade chord size on the cooling characteristics of air-cooled blades having corrugated inserts (ref. 5) indicated that, when the blade chord is less than 1 inch, the coolant-flow requirements increase rapidly, being as much as $2\frac{1}{2}$ times as great for a 1/2-inch as for a 1-inch-chord blade. Also, the coolant pressure losses in small passages may become large and the blade may be unable to pass the required airflow at the pressure levels available in engine operation (ref. 5). In addition, fabrication of small air-cooled blades presents problems because of the physical dimensions involved. Although several methods of fabricating air-cooled turbine blades for turbojet engines have been evolved (refs. 6 to 9), it is possible that these methods cannot be scaled and suitably applied to turboprop turbine blades.

Because of the problems associated with the cooling of turbine blades in turboprop engines, the NACA Lewis laboratory has initiated a program for investigating cooled turboprop turbine blades. One of the purposes of this report is to present the initial cooling results obtained on the first air-cooled turboprop turbine blade to be designed, fabricated, and tested at the Lewis laboratory. Another objective is to present a method for correlation of the data to permit its use at other than test conditions.

The blade configuration investigated has a span and chord of 1.4 and 0.7 inch, respectively. The blade was fabricated from two main components: One an integrally cast base, the airfoil suction surface, and the cooling fins; and the other a formed sheet-metal pressure surface. The cooling characteristics of this blade configuration were determined in a static cascade test facility that accommodated nine blades. Three cooled blades were instrumented with thermocouples and investigated at combustion-gas temperatures of about 1060°, 1360°, and 1660° R. The gas Reynolds number ranged from about 70,000 to 170,000. The blade cooling-air temperatures ranged from 580° to 1060° R, and the cooling-air Reynolds number from about 2400 to 21,600.

SYMBOLS

A	blade cooling-airflow passage area, sq ft
b	effective fin length, ft
$C_1, C_2 \dots C_{20}$	constants
c_p	specific heat at constant pressure, Btu/(lb)(°R)
d_h	hydraulic diameter (4 X flow area)/(wetted perimeter), ft
F	constant, function of blade transition ratio and Euler number
$f_1, f_2 \dots f_6$	functions
g	acceleration due to gravity, ft/sec ²
h	heat-transfer coefficient, Btu/(sec)(sq ft)(°R)
h_f	effective inside heat-transfer coefficient, Btu/(sec)(sq ft)(°R)
k	thermal conductivity, Btu/(sec)(°R)(ft)
L	length of blade or passage, ft
l	blade wall perimeter, ft
m	exponent, function of blade transition ratio and Euler number
N	number of fins
Nu	Nusselt number, hd_h/k
n	number of sections of equivalent fins
Pr	Prandtl number, $gc_p\mu/k$
Re	Reynolds number, $\rho V d_h/\mu g$
St	Stanton number, $Nu/PrRe$
s	fin spacing, ft

- T temperature, °R
 V velocity, ft/sec
 w weight-flow rate, lb/sec
 x distance from blade platform to blade element, ft

$$z_L f_1 \left[\frac{(\overline{Re}_{g,b})^{0.7}}{\overline{Re}_a} \left(\frac{\overline{T}_b}{\overline{T}_a} \right)^{0.85} \right]$$

$$z_T \frac{(\overline{Re}_{g,b})^{0.7}}{(\overline{Re}_a)^{0.8}} \left(\frac{\overline{T}_b}{\overline{T}_a} \right)^{1.25}$$

$$z_L f_6 \left[\frac{(\overline{Re}_{g,b})^{0.7}}{\overline{Re}_{a,i}} \left(\frac{\overline{T}_b}{\overline{T}_{a,i}} \right)^{0.85} \right]$$

$$z_T \frac{(\overline{Re}_{g,b})^{0.7}}{(\overline{Re}_{a,i})^{0.8}} \left(\frac{\overline{T}_b}{\overline{T}_{a,i}} \right)^{1.25}$$

$$\lambda \frac{\overline{h}_g \overline{l}_g}{\overline{h}_f \overline{l}_a}$$

μ viscosity, (lb)(sec)/sq ft

ρ density, lb/cu ft

τ fin thickness, ft

ϕ temperature-difference ratio, $(T_{g,e} - T_b)/(T_{g,e} - T_{a,i})$

Subscripts:

- a cooling air or cooling-air side
 b blade
 e effective
 g combustion gas or combustion-gas side

i inlet
L laminar flow
o outlet
T turbulent flow
 ξ index of summation
• fully established flow, cooling air

Superscripts:

- average conditions at particular span location
= average conditions for entire blade

APPARATUS

Blades

The size of the turboprop turbine blades selected for investigation (span of about 1.4 in. and chord of about 0.7 in.) is representative of that of turbine blades used in the first-stage turbines of present-day turboprop engines with a shaft-power output of about 3000 horsepower. Smaller turboprop engines (on the order of 1000 hp) would probably have blades of this size in the second-stage turbine. The airfoil shape of the cooled blade is the same as that employed in a current uncooled commercial turboprop engine.

Air is selected as the coolant because considerably more experience has been obtained at the Lewis laboratory with air-cooled turbojet-engine blades than with liquid-cooled blades. It is felt that much of this background in air-cooling (refs. 1 and 2, e.g.) is also applicable to the design, fabrication, and operation of air-cooled turboprop blades.

The blade configuration selected for investigation was fabricated in two main parts as shown in figure 1(a): one includes an integrally cast base, the airfoil suction surface, and the cooling fins; and the other a formed sheet-metal pressure surface. The cast part of the blade is made of HS-31, and the formed sheet metal of HS-25. The formed sheet-metal shell was furnace-brazed in the recesses at the leading- and trailing-edge regions of the blades to several of the cast cooling fins (fig. 2) and to the base in the root region of the blade with a commercial brazing compound. The base was then ground to the shape necessary to accommodate the blade in the cascade test section. The completed blade is shown in figure 1(b).

Several cross-sectional views of the blade airfoil are shown in figure 2. Ten 0.020-inch-thick cooling fins spaced 0.020 inch apart were cast integrally with the suction surface. The third, sixth, and ninth fins from the leading edge are 0.010 inch longer than the others and are designated primary fins; the shorter fins are hereinafter called secondary fins. The purpose of the primary fins is to provide intermediate support members to which the 0.010-inch-thick sheet-metal pressure-surface shell is brazed. In the root region (about 0.10 in. above base platform, fig. 2(c)), the maximum thickness of the cast wall between the base of the fins and the outer surface of the blade is in the midchord region and is about 0.070 inch. The thickness of the suction-surface wall decreases linearly from the value of 0.070 inch at the root section to 0.015 inch at the midspan position (fig. 2(b)). Also at the midspan position the suction-surface wall thickness is essentially constant in a chordwise direction, decreasing slightly in thickness only near the leading and trailing edges. The wall is not tapered from the midspan to the tip (figs. 2(a) and (b)).

All the fins terminate about 1 inch from the blade platform, except the sixth fin from the leading edge, which is a primary fin (see fig. 1(a)). This remaining primary fin extends to the tip of the blade and acts as the only support member (other than the leading and trailing edges) for the sheet-metal shell in the tip region of the blade (see fig. 2(a)). Most of the fins are terminated at the 1-inch-span position so that the coolant-flow area at the tip will not be reduced excessively. With this arrangement the free-flow areas of the coolant passages at the root, midspan, and tip are 0.017, 0.016, and 0.009 square inch, respectively. Eliminating most of the fins in the tip region of the blade reduces the cooling effectiveness in this region. In actual engine operation, however, this region of the blade will not be highly stressed; therefore the lower cooling effectiveness can probably be tolerated.

This cooled-blade configuration is a variation of the air-cooled strut-supported blade for turbojet engines discussed in references 7 and 9. The purpose of the secondary fins is to augment the surface area of the coolant passages. In this blade configuration the secondary fins improve removal of heat from the cast portion of the blade, which is the main support member. The clearance between the sheet-metal shell on the pressure surface and the secondary fins keeps the heat flow from the sheet-metal shell to the cast portion of the blade at a minimum. This may result in a relatively hot pressure surface; but this should be permissible, since the sheet-metal shell is not the primary load-carrying member of the blade.

Test Facility

In the test facility, combustion air passed successively through a measuring orifice, a combustion chamber, a plenum chamber, the test

section, and into the exhaust system. A standard jet-engine combustion chamber was used in order to obtain temperatures of the combustion air from 1060° to 1660° R. The inlet to the test section was equipped with a gradually converging duct to provide a uniform velocity profile at the cascade entrance. The blade cooling air passed through a filter, a pressure regulator, and a rotameter to the test blades.

The test section (fig. 3) consisted of a cascade of nine blades, of which only the middle three blades were instrumented and cooled. The nine blades were inserted in a holder that provided for removal of the entire unit from the test section for thermocouple repair if necessary. The holder had flow passages for the cooling air and openings through which the thermocouple leads from the blades were passed. All the joints between the blades, the holder, and the test section were sealed with ceramic cement to eliminate or reduce cooling-air leakage into the test section. A top view of the gas passage shows the blades and holder in place (fig. 4). The cascade was so oriented in the passage as to provide a zero angle of incidence of the gas relative to the blade midspan section. The deviation from a zero angle of incidence at other than the midspan position of the blades (approx. $\pm 10^\circ$) was assumed to have a negligible effect on the heat-transfer data (ref. 10).

The top wall of the gas passage (fig. 3) was an adjustable machined plate. The plate was made adjustable in order to permit testing blades of various lengths and also to allow variations in tip clearance. The tip clearance for the blades in the present investigation was 0.030 inch, which corresponds to the clearance of the conventional uncooled blades in an engine.

The air plenum chamber (inside diam., 4.7 in.) was large enough to permit insertion or removal of the blades and blade holder from the test section. In order to reduce the heat conduction into the cooling-air plenum chamber, a layer of insulating material was cemented to the under side of the gas-passage bottom wall within the air chamber. At the entrance the cement was faired in to provide a smooth entrance for the cooling air (fig. 3).

Instrumentation

Blades. - Eighteen thermocouples, six in each blade, were installed in the test blades at the locations shown in figure 2. These locations correspond approximately to the root, midspan, and tip. The blades were instrumented by cementing thermocouples made of 36-gage (0.005-in.-diam.) Chromel-Alumel wire in shallow (approx. 0.008 in. deep) grooves in the surface of the blade. Reference 11 describes in more detail the method of installing these small leads in thin-walled blades. The outputs of the thermocouples were read from a calibrated potentiometer.

Cascade. - The instrumentation of the cascade, shown schematically in figure 3, was such as to provide information for the reduction of the data to dimensionless parameters so that the data can be used at conditions other than those of this investigation.

Before the actual heat-transfer investigation, the gas-flow direction and the total-pressure distribution in a plane about 1/4 inch ahead of the three test blades were obtained with a probe that measured flow angle and total pressure. Because of space limitation, only one probe was used; it was moved to various transverse positions by use of suitably spaced holes in the top wall of the gas passage. After the survey of the gas passage, this probe was removed from the cascade and not used further. Instead, three fixed total-pressure probes were inserted at the mid-height of the gas passage. Also located at the mid-height (7.6 in. ahead of the blades) was a total-temperature rake having five open-end Chromel-Alumel probes equally spaced across the passage. Seven static-pressure wall taps were located across the gas passage in the bottom wall, 1 inch ahead of the cascade. Four static-pressure taps were also located at the exit of the cascade of blades in the adjustable wall of the gas passage.

The instrumentation in the cooling-air plenum chamber (fig. 3) consisted of four static taps equally spaced around the chamber wall and two open-end thermocouple probes approximately 0.5 inch from the entrance to the cooled blades. The cooling airflow and the cooling-air leakage flow (obtained by a calibration described in the next section) were measured by rotameters.

EXPERIMENTAL PROCEDURE

Gas-Flow Conditions in Cascade

Before determining the heat-transfer characteristics of the cooled blades, it was necessary to calibrate the cascade and to determine the flow characteristics of the hot gases. This calibration indicated that a single total-pressure probe ahead of each of the test blades would produce total-pressure readings proportional to the average total pressure ahead of the blades.

Blade Cooling Characteristics

The cooling characteristics of the blades were obtained by measuring the temperatures of the blades over a range of cooling airflows, gas flows, gas densities, and gas temperatures. The procedure for testing the blades was to set the gas conditions and then measure the blade temperatures, starting with no cooling airflow to the blades and then

increasing the cooling airflow in steps until the flow in the coolant passages was approximately choked. The gas-flow conditions were then changed and the procedure was repeated. The gas flows per unit flow area ahead of the three test blades ranged from 24 to 53 pounds per second per square foot. This range of flows corrected to static sea-level conditions varied from 34 to 36 pounds per second per square foot. The ratio of cooling-air to combustion-gas flow ranged from 0 to about 0.03. The tests were conducted at three gas-temperature levels: 1060°, 1360°, and 1660° R.

Leakage calibrations were made at the start and finish of a series of test runs at each gas-temperature level by capping and sealing the tips of the test blades with gasket material so that no cooling air could flow from the blade tip. The leakage from the base joints was then determined for the required range of cooling-air pressure differences between the blade cooling-air inlet and the static pressure in the combustion-gas passage ahead of the blades (see fig. 3).

The leakage at the start of a series of test runs was a maximum of 8.1 percent of the cooling air supplied and increased to a maximum of 9.6 percent at the conclusion of the series of test runs. A curve of the mean leakage (leakage at start of series of tests plus leakage at conclusion of tests divided by 2) was plotted against the static-pressure differences and used for determining the actual coolant flow through the test blades for each series of tests at a given combustion-gas temperature.

CALCULATION PROCEDURE

Correlation of Cooled-Blade Temperatures

The data of the investigation are not presented on an absolute basis, but rather are correlated with dimensionless parameters to permit more general use. The actual blade temperatures are not presented, because the low blade metal temperatures at which the tests were made (because of the temperature limitations of existing test equipment) are not representative of those that exist in practical engine operation. The blade temperature is correlated by using an approximate equation to determine the spanwise temperature distribution of a blade shell (ref. 12). Neglecting the terms relating to the rotation of the blades, the equation in the notation of the present report is

$$\bar{\phi} = \frac{\bar{T}_{g,e} - \bar{T}_b}{\bar{T}_{g,e} - T_{a,i}} = \frac{1}{1 + \lambda} \exp \left[\left(\frac{1}{1 + \lambda} \right) \frac{\bar{h}_g x}{c_{p,a} (w_a / \bar{l}_g)} \right] \quad (1)$$

where $\lambda = \bar{h}_g \bar{l}_g / \bar{h}_f \bar{l}_a$.

The gas-to-blade heat-transfer coefficient \bar{h}_g is obtained from the correlation equation of reference 13:

$$\bar{Nu}_g = F(\bar{Re}_{g,b})^m (\bar{Pr}_{g,b})^{1/3} \quad (2)$$

where $F = 0.092$ and $m = 0.70$. The values of F and m , which were obtained from reference 14, are the average values of ten rotor blade profiles including both impulse and reaction blades. For a given blade geometry, equation (2) can be reduced to

$$\bar{h}_g = C_1 (\bar{Re}_{g,b})^{0.7} (\bar{Pr}_{g,b})^{1/3} \bar{k}_{g,b} \quad (3)$$

The blade-to-air heat-transfer coefficient \bar{h}_a is obtained from correlation equations for flow through rectangular tubes (ref. 15). In the notation of this report, the equations for turbulent and laminar flow are, respectively,

$$\bar{St}_a (\bar{Pr}_a)^{2/3} = 0.02 (\bar{Re}_a)^{-0.2} \frac{\bar{T}_b}{\bar{T}_a}^{-0.4} \left(1 + \frac{3.8}{L/\bar{d}_h} \right) \quad (4)$$

and

$$\frac{\bar{Nu}_a}{Nu_\infty} = 1 + \left(\frac{C_2 \bar{Re}_a \bar{Pr}_a}{L/\bar{d}_h} \right) \quad (5)$$

For a blade in which the internal coolant configuration can be replaced by equivalent fins (ref. 16), the equation for the effective blade-to-air heat-transfer coefficient may be written as follows:

$$\bar{h}_f = \sum_{\zeta=1}^n \frac{\bar{h}_a}{N_\zeta (s_\zeta + \tau_\zeta)} \left[\sum_{\zeta=1}^n \frac{N_\zeta 2b_\zeta \tanh \left(b \sqrt{2\bar{h}_a/\bar{k}_a} / \zeta \right)}{\left(b \sqrt{2\bar{h}_a/\bar{k}_a} / \zeta \right)_\zeta} + \sum_{\zeta=1}^n N_\zeta s_\zeta \right] \quad (6)$$

This equation, for typical internal blade configurations (ref. 16), including that for the test blade herein, can be reduced to

$$\bar{h}_f = C_3 \bar{h}_a \quad (7)$$

Then, for a specified blade (fixed geometry), equations (4) to (7) combine to give the following equations for turbulent and laminar flow, respectively:

$$\bar{h}_{f,T} = C_4 (\overline{Re}_a)^{0.8} \left(\frac{\overline{T}_a}{\overline{T}_b} \right)^{0.4} (\overline{Pr}_a)^{1/3} \bar{k}_a \quad (8)$$

and

$$\bar{h}_{f,L} = C_5 (1 + C_6 \overline{Re}_a \overline{Pr}_a) \bar{k}_a \quad (9)$$

By writing the fluid properties of the combustion gas based on blade temperatures from 800° to 2200° R and of the cooling air based on bulk temperatures from 600° to 1200° R as

$$\overline{Pr}_a = C_7, \quad \overline{Pr}_{g,b} = C_8$$

and

$$\bar{k}_a = C_9 (\overline{T}_a)^{0.85}, \quad \bar{k}_{g,b} = C_{10} (\overline{T}_b)^{0.85}$$

and substituting in equations (3), (8), and (9), the following expressions can be obtained:

$$\bar{h}_g = C_{11} (\overline{Re}_{g,b})^{0.7} (\overline{T}_b)^{0.85} \quad (10)$$

$$\bar{h}_{f,T} = C_{12} \frac{C_{12} (\overline{Re}_a)^{0.8} (\overline{T}_a)^{1.25}}{(\overline{T}_b)^{0.4}} \quad (11)$$

$$\bar{h}_{f,L} = (C_{13} + C_{14} \overline{Re}_a) (\overline{T}_a)^{0.85} \quad (12)$$

By substituting equations (10), (11), and (12) into equation (1) and assuming that $c_{p,a} = C_{15} (\overline{T}_a)^{0.06}$ and $\mu_a = C_{16} (\overline{T}_a)^{0.7}$ for the range of cooling-air temperatures from 600° to 1200° R, the following relations are obtained for turbulent and laminar flow, respectively:

$$\bar{\phi} = \left(\frac{1}{1 + C_{17} Z_T} \right) \exp \left\{ - \left(\frac{C_{18} Z_T}{1 + C_{17} Z_T} \right) \left[\frac{(\overline{T}_a)^{0.49} / (\overline{T}_b)^{0.4}}{(\overline{Re}_a)^{0.2}} \right]^x \right\} \quad (13)$$

$$\bar{\phi} = \left(\frac{1}{1 + C_{19}Z_L} \right) \exp \left[- \left(\frac{C_{18}Z_L}{1 + C_{19}Z_L} \right) (\bar{T}_a)^{0.9} x \right] \quad (14)$$

where

$$Z_T = \frac{(\bar{Re}_{g,b})^{0.7} (\bar{T}_b)^{1.25}}{(\bar{Re}_a)^{0.8} (\bar{T}_a)}$$

and

$$Z_L = \frac{(\bar{Re}_{g,b})^{0.7} (\bar{T}_b)^{0.85}}{C_{13} + C_{14}\bar{Re}_a (\bar{T}_a)} = f_1 \left[\frac{(\bar{Re}_{g,b})^{0.7} (\bar{T}_b)^{0.85}}{\bar{Re}_a (\bar{T}_a)} \right]$$

Since the second term in the exponential of equations (13) and (14) at any given value of Z does not vary appreciably, the terms are assumed constant; therefore, for any span position,

$$\bar{\phi} = f_2(Z_T) \quad (15)$$

$$\bar{\phi} = f_3(Z_L) \quad (16)$$

By assuming that the air temperature and Reynolds number terms in the parameters Z_T and Z_L vary as a function of distance along the span, the equations are converted to the form used to correlate the heat-transfer data presented in this report:

$$\bar{\phi} = f_4(z_T) \quad (17)$$

$$\bar{\phi} = f_5(z_L) \quad (18)$$

where

$$z_T = \frac{(\bar{Re}_{g,b})^{0.7} (\bar{T}_b)^{1.25}}{(\bar{Re}_{a,i})^{0.8} (\bar{T}_{a,i})}$$

and

$$z_L = f_6 \left[\frac{(\bar{Re}_{g,b})^{0.7} (\bar{T}_b)^{0.85}}{\bar{Re}_{a,i} (\bar{T}_{a,i})} \right]$$

Parameters for Correlating Blade Temperatures

Effective gas temperature. - The effective gas temperature $\bar{T}_{g,e}$ (or the temperature that an uncooled blade in the gas stream would attain) at the blade root, midspan, and tip is the arithmetic average of the temperature readings indicated by the six thermocouples at each of these locations (fig. 2) with no cooling air flowing.

Cooled-blade temperatures. - The temperature of the cooled-blade metal \bar{T}_b at the root, midspan, and tip is obtained with the same thermocouples and in the same manner as the effective gas temperature. The blade temperature \bar{T}_b is the arithmetic average of the eighteen thermocouples on the blades.

Cooling-air inlet temperature. - The cooling-air temperature at the inlet to the blades $T_{a,i}$ is the arithmetic average of two thermocouples located at the blade entrance (fig. 3).

Cooling-air inlet Reynolds number. - The cooling-air inlet Reynolds number $Re_{a,i}$ is obtained from the equation

$$Re_{a,i} = \frac{w_a d_{n,a,i}}{A_{a,i} \mu_{a,i} g} \quad (19)$$

The viscosity term is evaluated at the measured air inlet temperature $T_{a,i}$.

Gas Reynolds number. - The gas Reynolds number $\bar{Re}_{g,b}$ is the arithmetic average of the Reynolds numbers at the inlet and exit of the cascade.

Inlet gas Reynolds number: The inlet gas Reynolds number $\bar{Re}_{g,b,i}$ is calculated from the equation

$$Re_{g,b,i} = \frac{\bar{V}_{g,i} \bar{\rho}_{g,b,i} \bar{d}_{n,g}}{\mu_{g,b,i} g} \quad (20)$$

The average gas inlet velocity $\bar{V}_{g,i}$ is determined by the use of a proportionality constant that relates the velocity at the midspan of the blades to the average of the spanwise velocity distribution. The midspan velocity measurements are obtained by use of the ratio of static to total gas pressure and the total gas temperature at the inlet. The gas total temperature is the arithmetic average of the five thermocouple readings across the gas passage (fig. 3). The total pressure is the

arithmetic average of the three fixed probes ahead of the test blades. The static pressure is the arithmetic average of the three static taps located in the floor of the gas passage ahead of the test blades. It is assumed that no static-pressure gradient existed along the height of the gas passage so that the static pressure at the wall is the average of the passage. The average velocity $\bar{V}_{g,i}$ is then calculated from

$$\bar{V}_{g,i} = C_{20} \bar{V}_{g,i} \quad (21)$$

where the constant of proportionality C_{20} is 0.96.

The density term of equation (20) is solved by use of the average static pressure and the blade temperature T_b . The viscosity $\mu_{g,b,i}$ is evaluated at the same blade temperature.

Outlet gas Reynolds number: The outlet gas Reynolds number $\bar{Re}_{g,b,o}$ is obtained with the same terms as equation (20), except that the values of the terms are obtained at the exit of the blades.

With the assumption that the heat and friction losses across the blade are negligible, the average exit velocity $\bar{V}_{g,o}$ is calculated with the use of the inlet values of the total gas temperature and pressure and the exit value of gas static pressure. The static gas pressure used is the arithmetic average of four static taps located in the top of the gas passage and at the cascade exit in the center of gas passages between the test blades.

The density of the gas at the outlet $\bar{\rho}_{g,b,o}$ is calculated from the average exit static pressure and the blade temperature T_b .

RESULTS AND DISCUSSION

Gas-Flow Conditions in Cascade Test Section

As discussed previously in the EXPERIMENTAL PROCEDURE, the combustion-gas flow conditions in the test section of the cascade were determined before test data were taken. The results of pressure and temperature surveys in the gas-flow passage upstream of the test blades indicate that the velocity ahead of the three test blades was essentially constant in both vertical and horizontal directions for the entire range of combustion-gas flows. The maximum boundary-layer thickness at the top and bottom of the cascade was less than 0.1 and 0.2 inch, respectively. The maximum angular deviation of the flow from a plane parallel to the cascade walls was $\pm 3^\circ$. These varying flow conditions do not significantly influence the cooling characteristics of the

blades (ref. 10). The survey data also show that the proportionality constant C_{20} used in equation (21) and discussed in the CALCULATION PROCEDURE is 0.96 (± 2 percent). This value of C_{20} relates the value of velocity at the midspan of the blades to the average velocity immediately upstream of the blades.

Correlation of Temperature Data

In the CALCULATION PROCEDURE two correlation equations (eqs. (17) and (18)) were derived for application when the cooling-air Reynolds number at the inlet to the cooled turbine blades is either in turbulent or laminar flow. For the range of coolant flows investigated herein, the coolant-flow Reynolds number at the blade inlet ranged from about 2400 to about 21,600. Since these values of Reynolds number indicate that the flow is either in the transition or turbulent flow range, the correlation of the data is attempted by use of the correlation parameter for turbulent flow; that is,

$$\bar{\phi} = f_4(z_T) = f_4 \left[\frac{(\overline{Re}_{g,b})^{0.7} (\bar{T}_b)^{1.25}}{(\overline{Re}_{a,i})^{0.8} (\bar{T}_{a,i})} \right]$$

Blade temperature at a particular span location. - The experimental heat-transfer data (a tabulation of typical conditions is shown in table I) were correlated by plotting the temperature parameter $\bar{\phi}$ against the parameter z_T for the blade root, midspan, and tip locations as shown in figure 5. The data correlate well about mean lines through the data. The value of the temperature parameter $\bar{\phi}$ at the root, midspan, and tip correlates within about 5, 6, and 12 percent, respectively. This deviation of the $\bar{\phi}$ data from the mean line corresponds to a maximum deviation in blade temperatures of about 15° R.

Average blade temperature. - Since the data for a particular span location correlated well, the average blade temperature data should also correlate, because the spanwise $\bar{\phi}$ distributions are approximately linear. The correlation of the average blade temperatures is therefore attempted by plotting the parameter $\bar{\bar{\phi}}$, defined as $(\bar{T}_{g,e} - \bar{T}_b) / (\bar{T}_{g,e} - \bar{T}_{a,i})$, against the parameter z_T (fig. 6). The use of the average parameters $\bar{\bar{\phi}}$ and z_T correlates all the data about a mean line within approximately 7 percent.

Local blade temperature. - The parameter z_T includes terms that are generally related to blade metal temperature. Therefore, correlation of the local blade temperature was attempted by plotting at constant

values of z_T the parameter ϕ , defined as $(T_{g,e} - T_b)/(T_{g,e} - T_{a,i})$, against peripheral locations around the blade. The plots were made at approximate value of the parameter z_T for which at least three data points were available. A typical variation of the local correlated blade temperatures is shown in figure 7 for a value of z_T equal to approximately 6.9; the reason for selecting this particular value for presentation of the local correlation data is discussed in the next section. The values of the terms in the correlating parameter for each of test conditions considered are tabulated in the figure. The maximum deviation of the data from the curve in figure 7 is about ± 7 percent. This represents a deviation in blade metal temperature of about $\pm 6^\circ$ R at the blade tip and about $\pm 15^\circ$ R at the blade base. Because of failure of several of the thermocouples on the pressure surface in the root region of the blade, the variation of ϕ at the root is estimated to be similar to that observed at the midspan and tip of the blade.

Local correlation curves similar to those shown in figure 7 were obtained for the entire range of values of z_T , but they are not presented herein. In most instances the maximum variation of individual data points from a curve representing an approximate average of all the data was of the same order as that shown on figure 7; that is, ± 7 percent.

Application of Correlated Data to Typical Engine

Correlated average blade metal temperatures. - Since the heat-transfer characteristics of the blades correlate satisfactorily, the data were used to determine the cooled-blade temperatures at conditions other than those of the cascade tests. The conditions selected for an example are those of a typical turboprop engine operating (1) at zero flight speed at sea level and (2) at a speed of 300 knots at an altitude of 30,000 feet. A turbine-inlet gas temperature of 2460° R is assumed for both engine operating conditions. Table II lists some of the other engine conditions that are required in making the calculations. The gas-flow conditions relative to the first-stage-turbine rotor blades are determined from the assumed engine conditions. The cooling-air temperature at the blade entrance is obtained by assuming that the air is bled from the last stage of the compressor and that a 100° R rise in the air temperature results as the air is ducted from the compressor to the entrance of the turbine rotor blades. With the gas and cooling-air conditions relative to the blade known, the correlating parameter z_T is calculated for a range of ratios of blade cooling-air to combustion-gas flow w_a/w_g and average blade temperatures T_b . (Hereinafter the cooling-airflow to combustion-gas-flow ratio is referred to as the coolant-flow ratio.)

A plot of the correlating parameter against coolant-flow ratio is then made for the two engine conditions considered, as shown on the right side of figure 8. On the left side of figure 8 is plotted the line representing the correlated data of figure 6. In applying the same relation of $\bar{\phi}$ and z_T from the cascade data to an engine as in figure 8, the effects of rotation on the $\bar{\phi}$ and z_T relation are neglected. Calculations indicate that consideration of rotation would cause changes in the curve shown in figure 8 that would be within the spread of the data points of figure 6 from which the curve was originally drawn.

The required coolant-flow ratio for a desired average blade temperature can be determined by use of figure 8. A specific example is indicated in the figure by the dashed lines. A desired average blade temperature of 1985°R is selected for a flight condition of 30,000 feet and 300 knots. The resulting value of $\bar{\phi}$ is 0.278, and the associated value of z_T is 6.9. For an ordinate value of 6.9 and the selected engine operating conditions, the coolant-flow ratio is 0.015.

The required coolant-flow ratio for other average blade metal temperatures and engine operating conditions can be determined by the method just described. Curves such as those shown in figure 9 are obtained by using figure 8 and assuming a series of different average blade metal temperatures for the two engine conditions considered herein. Figure 9 shows that, for the range of average blade metal temperatures considered, the coolant-flow requirements are about the same for sea-level static and altitude flight operation. For average blade temperatures above about 1825°R , the altitude flight condition requires slightly more cooling air than the sea-level static operation. For blade metal temperatures below 1825°R , the relation between the coolant requirements of the sea-level and altitude conditions reverses. Figure 9 shows that, if average blade metal temperatures below about 1800°R were necessary, the coolant-flow requirements would increase rapidly relative to the amount of metal temperature reduction achieved. This would lead to excessive engine performance losses due to cooling requirements (refs. 1 and 3). It should be noted that the cooling-requirement trends shown in figure 9 are not necessarily typical of all cooled-blade configurations nor of all cooled turboprop engines; the relations between the curves can change with blade cooling characteristics and engine performance characteristics.

Correlated local blade metal temperatures. - Since the local values of the temperature-difference ratio ϕ around the periphery and along the span of the blade are also correlated by the parameter z_T , the blade temperature distribution at other than test conditions can be determined. The conditions used previously for the average blade temperature correlations are employed to illustrate the use of the correlated

local temperature data. For the required value of coolant-flow ratio of 0.015 and the assumed flight conditions used in the example of figure 8, the value of z_T is 6.9. The local values of ϕ are plotted for this value of z_T in figure 7. With the peripheral distribution of ϕ in figure 7 and the values of $T_{g,e}$ and $T_{a,i}$ for the assumed flight conditions, the local blade metal temperature distributions shown in figure 10 are obtained. A constant spanwise distribution of $T_{g,e}$ is assumed for this example. The resulting blade temperature distribution for the small blade investigated herein is approximately the same as that for larger turbojet-engine blades, such as those discussed in references 17 and 18, the temperature difference between the leading edge and the mid-chord region being about 250° R.

A method of evaluating the cooling effectiveness of turbojet blades (ref. 16) makes use of a factor called the stress-ratio factor, which is defined as the ratio of the allowable stress-rupture strength for the blade material and for a desired blade life to the calculated average centrifugal stress at the critical span region of the blade. The critical region is defined as the spanwise location in the blade airfoil at which a curve of the allowable spanwise blade temperature distribution is tangent to a curve of the measured or calculated spanwise blade temperature distribution. The critical location for the small turbine rotor blade for the assumed altitude flight conditions and a coolant-flow ratio of 0.015 is approximately at the midspan of the blade. The calculated centrifugal stress at this location is 6750 psi. The average blade metal temperature at this location is 2010° R. Assuming that a blade life of 1000 hours is desired and that the blade is made of a high-temperature alloy such as HS-31, the calculated stress-ratio factor for the blade is found to be about 3. This value of the stress-ratio factor appears adequate compared with results of experimental investigations of the durability of air-cooled turbojet-engine blades made of high-temperature alloy.

References 9 and 19 indicate that values of stress-ratio factor between about 1.2 to 1.5 may be adequate. The blades in these references were either investigated uncooled or with small quantities of cooling air, with the result that the peripheral temperature gradients and the resulting thermal stresses were small. The stress-ratio factors obtained are nevertheless indicative of the margin of safety required for cooled-blade configurations under engine test conditions. Since the stress-ratio factors presented in these references were based on average blade temperatures at a particular span location, local values of the stress-ratio factors at the hot leading and trailing edges would be less, assuming that the centrifugal-stress distribution across the blade chord is constant. For the small blade of this report, even with the high metal temperature at the leading edge, the stress-ratio factor

based on the temperature of the leading edge at the critical midchord location is about 1.63. This value is a more conservative local value than those of the turbojet blades of references 9 and 19. Based on the relatively conservative stress-ratio factors, a reasonably satisfactory blade life may be predicted for the air-cooled turbine blade configuration investigated herein.

SUMMARY OF RESULTS

The results of a static cascade investigation to determine the cooling effectiveness of a small air-cooled turbine blade intended for use in a turboprop engine are as follows:

1. A nondimensional method of correlating the experimental heat-transfer data of the blades was developed that correlated the blade temperatures with the gas and cooling-air conditions of the tests. The correlated data were within about 7 percent of a mean line drawn through the data. The correlation method is applicable to average blade temperatures at particular span locations, local metal temperatures, and the average metal temperatures of the entire blade.
2. Application of the correlated data to a typical turboprop engine operating at a turbine-inlet temperature of 2460° R either at sea-level static conditions or at 30,000 feet altitude and 300 knots revealed that appreciable cooling of the blades can be expected with small coolant-flow ratios. The average blade temperature at the altitude flight condition for a coolant-flow ratio of 0.015 was 1985° R.
3. At the altitude flight conditions the blade peripheral temperature distribution for the small blade was approximately the same as that obtained experimentally in the past for much larger turbojet-engine blades. The temperature difference between the leading edge and the midchord region of the blade was about 250° R.
4. The calculated stress-ratio factor for a 2460° R turbine-inlet temperature and a coolant-flow ratio of 0.015 was about 3. This value of stress-ratio factor appears adequate when compared with required values of about 1.2 to 1.5 determined from tests of larger air-cooled turbine blades intended for use in turbojet engines.

Lewis Flight Propulsion Laboratory
National Advisory Committee for Aeronautics
Cleveland, Ohio, April 22, 1957

REFERENCES

1. Esgar, Jack B., and Ziemer, Robert R.: Review of Status, Methods, and Potentials of Gas-Turbine Air-Cooling. NACA RM E54I23, 1955.
2. Esgar, J. B., Livingood, J. N. G., and Hickel, R. O.: Research on Application of Cooling to Gas Turbines. Paper No. 56-SA-54, ASME, 1956.
3. Esgar, Jack B., and Ziemer, Robert R.: Effect of Turbine Cooling with Compressor Air Bleed on Gas-Turbine Engine Performance. NACA RM E54L20, 1955.
4. Esgar, Jack B., and Slone, Henry O.: Gas-Turbine-Engine Performance When Heat from Liquid-Cooled Turbines Is Rejected Ahead of, Within, or Behind Main Compressor. NACA RM E56B09, 1956.
5. Esgar, Jack B., Schum, Eugene F., and Curren, Arthur N.: Effect of Chord Size on Weight and Cooling Characteristics of Air-Cooled Turbine Blades. NACA TN 3923, 1957.
6. Long, Roger A., and Esgar, Jack B.: Experimental Investigation of Air-Cooled Turbine Blades in Turbojet Engines. VII - Rotor-Blade Fabrication Procedures. NACA RM E51E23, 1951.
7. Schum, Eugene F., and Stepka, Francis S.: Analytical and Experimental Investigation of a Forced-Convection Air-Cooled Internal Strut-Supported Turbine Blade. NACA RM E53L22a, 1954.
8. Freche, John C., and Oldrieve, Robert E.: Fabrication Techniques and Heat-Transfer Results for Cast-Cored Air-Cooled Turbine Blades. NACA RM E56C06, 1956.
9. Schum, Eugene F., Stepka, Francis S., and Oldrieve, Robert E.: Fabrication and Endurance of Air-Cooled Strut-Supported Turbine Blades with Struts Cast of X-40 Alloy. NACA RM E56A12, 1956.
10. Ainley, D. G., Waldren, N. E., and Hughes, K.: Investigations on an Experimental Air-Cooled Turbine. II - Cooling Characteristics of Blades Having a Multiplicity of Small Diameter Coolant Passages. Rep. No. R.154, British NGTE, Mar. 1954.
11. Stepka, Francis S., and Hickel, Robert O.: Methods for Measuring Temperatures of Thin-Walled Gas-Turbine Blades. NACA RM E56G17, 1956.

- 4436
12. Livingood, John N. B., and Brown, W. Byron: Analysis of Spanwise Temperature Distribution in Three Types of Air-Cooled Turbine Blades. NACA Rep. 994, 1950. (Supersedes NACA RM's E7B11e and E7G30.)
 13. Brown, W. Byron, and Donoughe, Patrick L.: Extension of Boundary-Layer Heat-Transfer Theory to Cooled Turbine Blades. NACA RM E50F02, 1950.
 14. Donoughe, Patrick L.: Outside Heat Transfer of Bodies in Flow - A Comparison of Theory and Experiment. M.S. Thesis, Case Inst. Tech., 1951.
 15. Kays, W. M., and Clark, S. H.: A Summary of Basic Heat Transfer and Flow Friction Design Data for Plain Plate-Fin Heat Exchanger Surfaces. Tech. Rep. No. 17, Dept. Mech. Eng., Stanford Univ., Aug. 15, 1953. (Contract N6-ONR-251, Task Order 6 (NR-090-104) for Office Naval Res.)
 16. Ziemer, Robert R., and Slone, Henry O.: Analytical Procedures for Rapid Selection of Coolant Passage Configurations for Air-Cooled Turbine Rotor Blades and for Evaluation of Heat-Transfer, Strength, and Pressure-Loss Characteristics. NACA RM E52G18, 1952.
 17. Bartoo, Edward R., and Clure, John L.: Experimental Investigation of Air-Cooled Turbine Blades in Turbojet Engine. XII - Cooling Effectiveness of a Blade with an Insert and with Fins Made of a Continuous Corrugated Sheet. NACA RM E52F24, 1952.
 18. Stepka, Francis S., Bear, H. Robert, and Clure, John L.: Experimental Investigation of Air-Cooled Turbine Blades in Turbojet Engine. XIV - Endurance Evaluation of Shell-Supported Turbine Rotor Blades Made of Timken 17-22A(S) Steel. NACA RM E54F23a, 1954.
 19. Freche, John C., and Schum, Eugene F.: Cooling Performance and Structural Reliability of a Modified Corrugated-Insert Air-Cooled Turbine Blade with an Integrally Cast Shell and Base. NACA RM E56K09, 1957.

TABLE I. - TYPICAL CASCADE OPERATING CONDITIONS

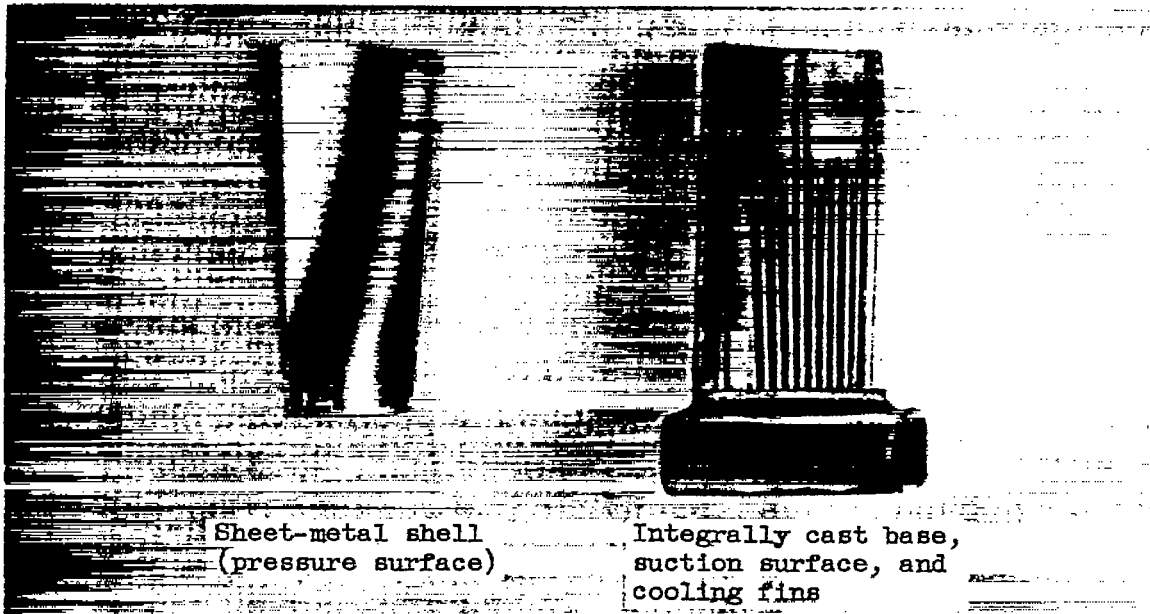
$\bar{T}_{g,e},$ $^{\circ}R$	$T_{a,i},$ $^{\circ}R$	$\bar{T}_b, ^{\circ}R$			$Re_{a,i} \times 10^{-4}$	$\bar{Re}_{g,b} \times 10^{-5}$
		Root	Midspan	Tip		
1311	639	875	954	1033	1.68	0.99
1311	700	948	1041	1112	1.07	.88
1311	802	1060	1160	1219	.24	.75
1619	668	999	1126	1242	1.61	.88
1619	754	1099	1225	1339	.96	.86
1619	953	1296	1441	1522	.39	.66

TABLE II. - ASSUMED ENGINE AND FLIGHT CONDITIONS

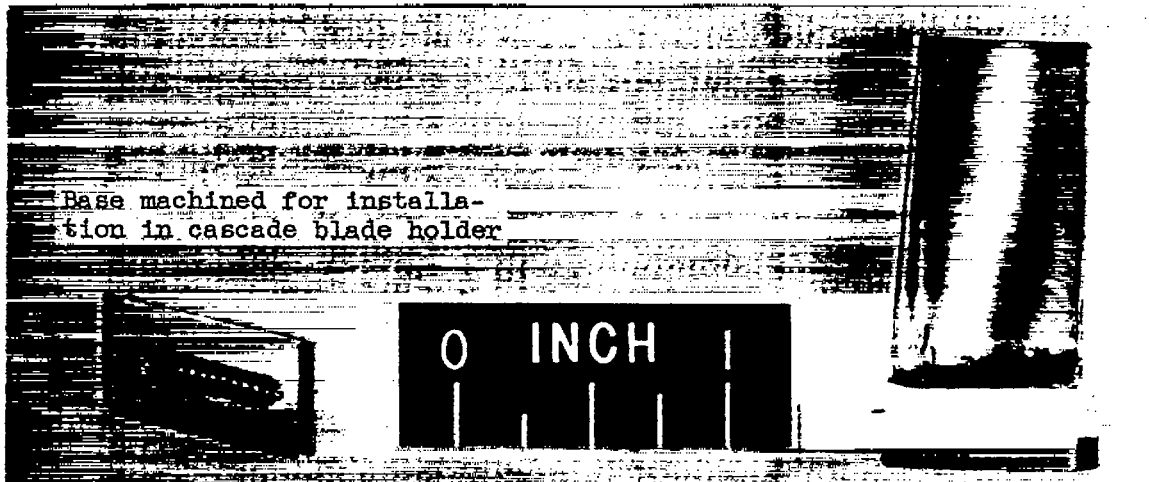
[Combustor pressure ratio, 0.95; turbine-inlet temperature, 2460 $^{\circ}$ R; turbine efficiency, 0.85; exhaust-nozzle pressure ratio, 0.92.]

Altitude, ft	Sea level	30,000
Flight speed, knots	0	300
Compressor pressure ratio	9.4	10.88
Compressor airflow, lb/sec	32.5	13.4
Compressor efficiency	0.84	0.77
Av. effective gas temp., $^{\circ}R$	2335	2331
Blade cooling-air inlet temp., $^{\circ}R$	1173	1083

4436



(a) Blade before assembly.



(b) Assembled blade.

C-44787

Figure 1. - Blade components before and after assembly.

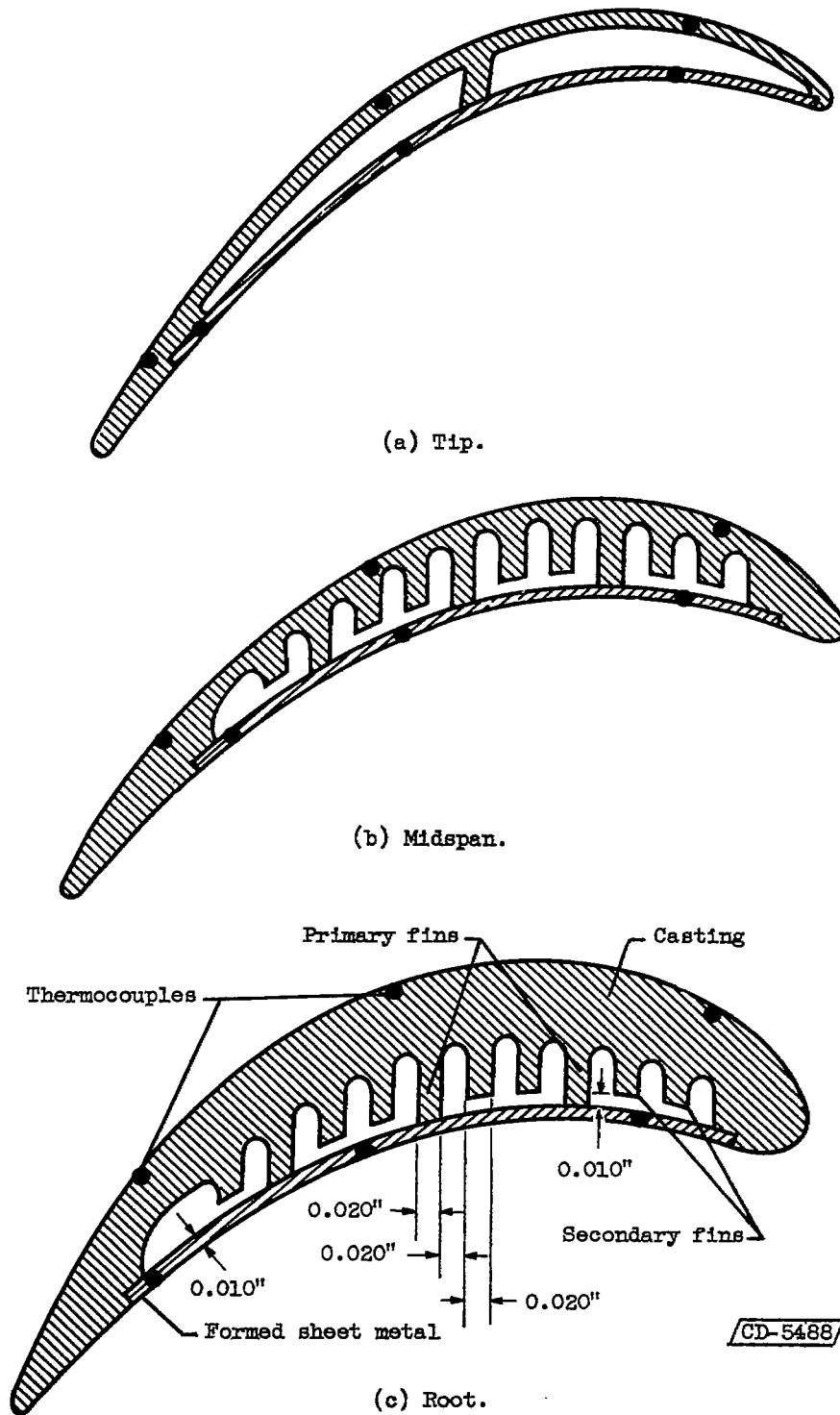
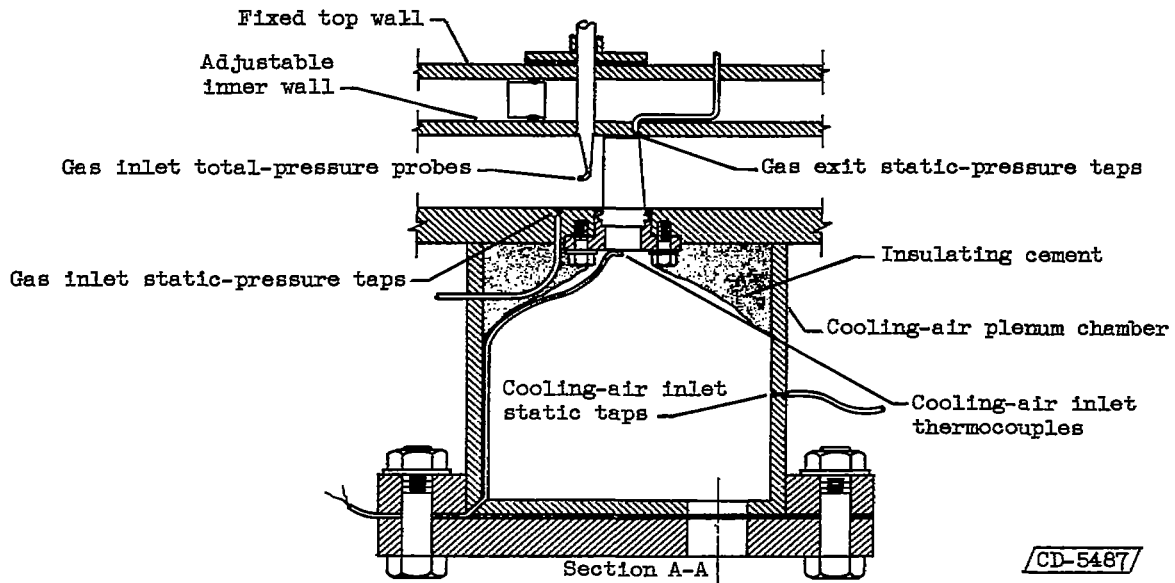
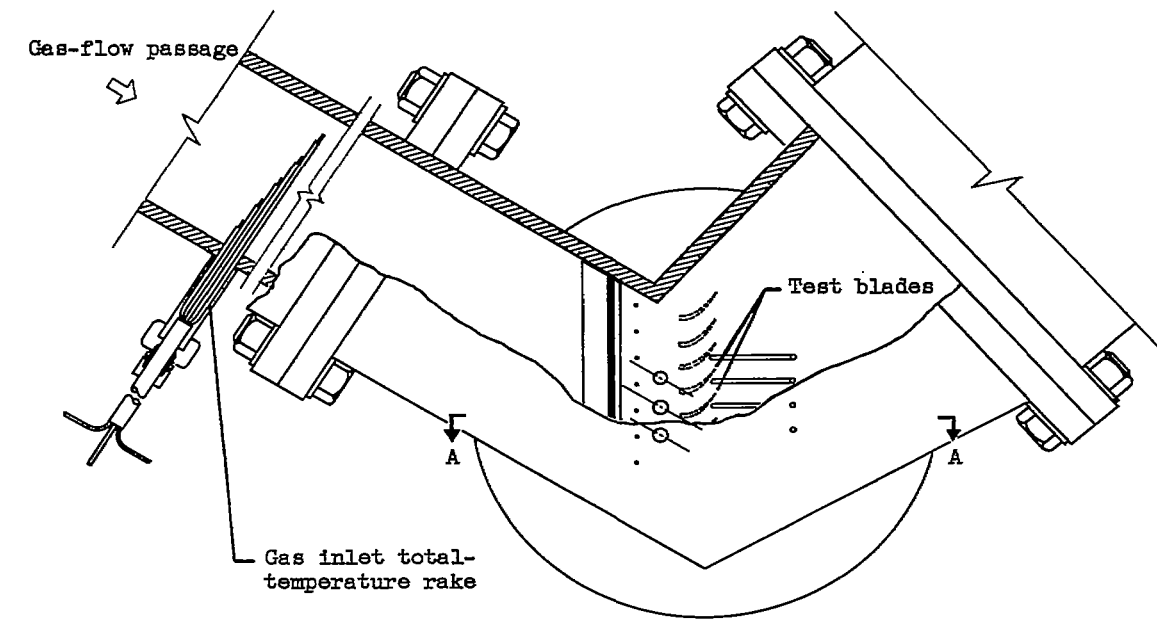


Figure 2. - Cross-sectional views of internally firmed turboprop blade at approximately the root, midspan, and tip locations.

4436

CI-4



CD-5487

Figure 3. - Cascade test section with instrumentation.

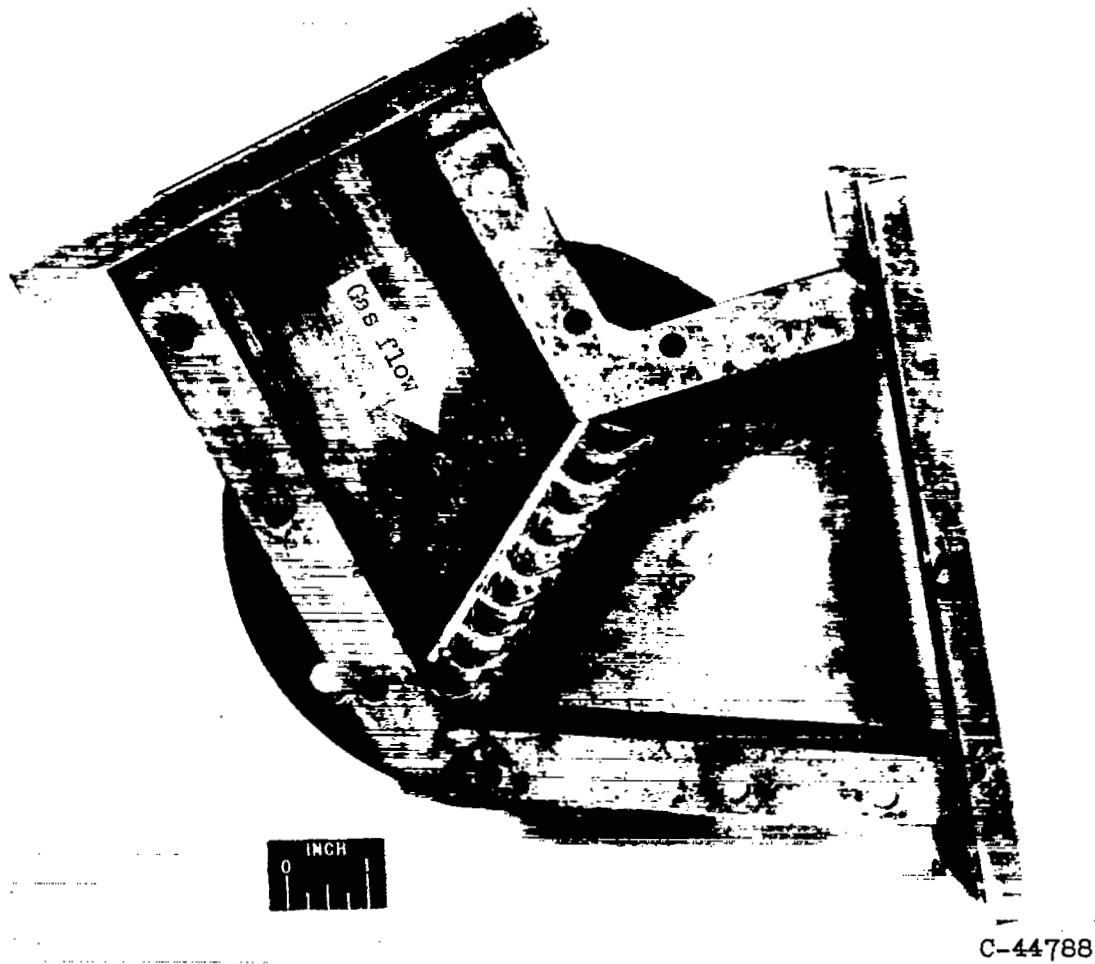


Figure 4. - Top view of cascade test section.

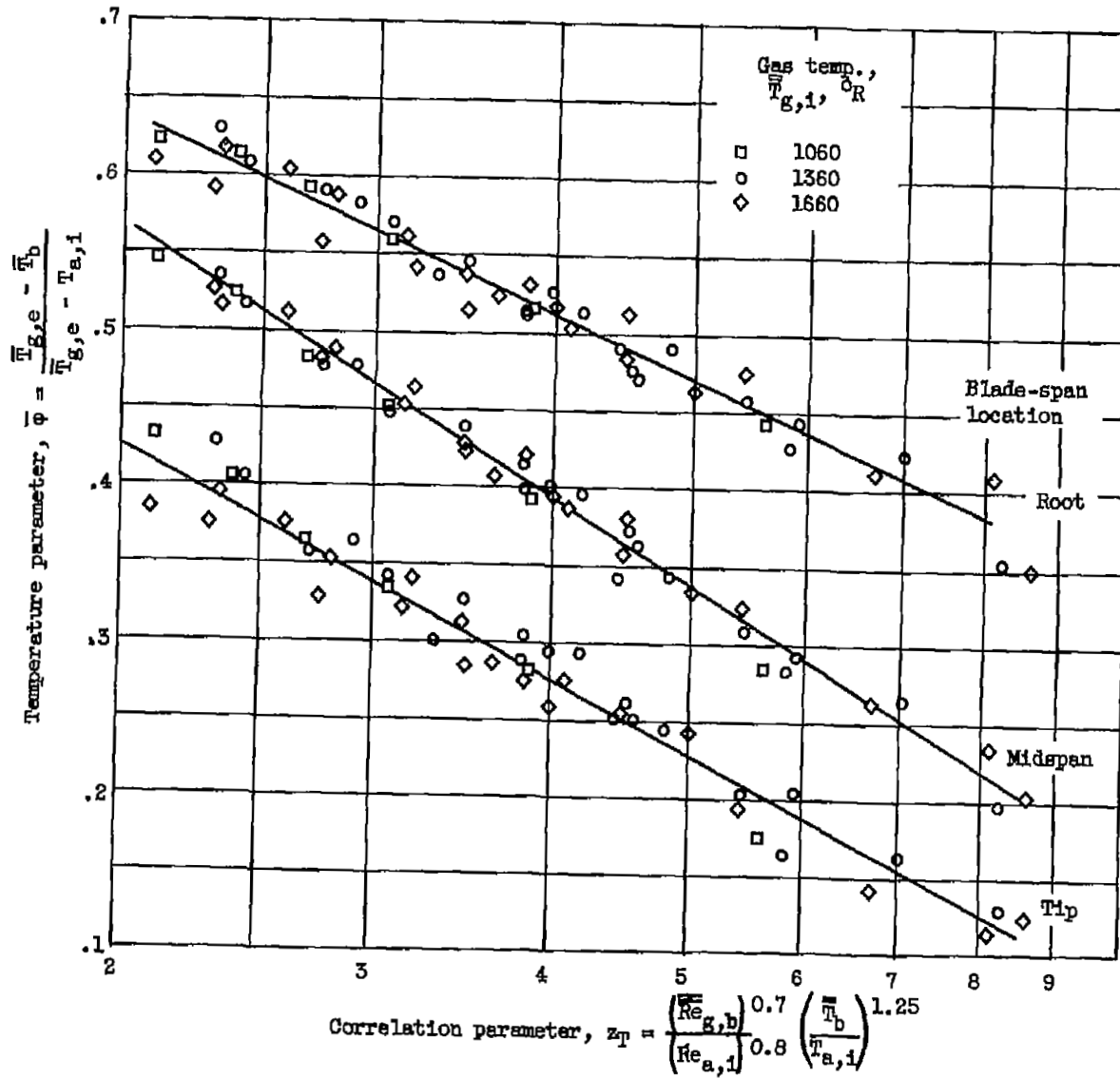


Figure 5, - Correlation of blade metal temperatures at particular span locations.

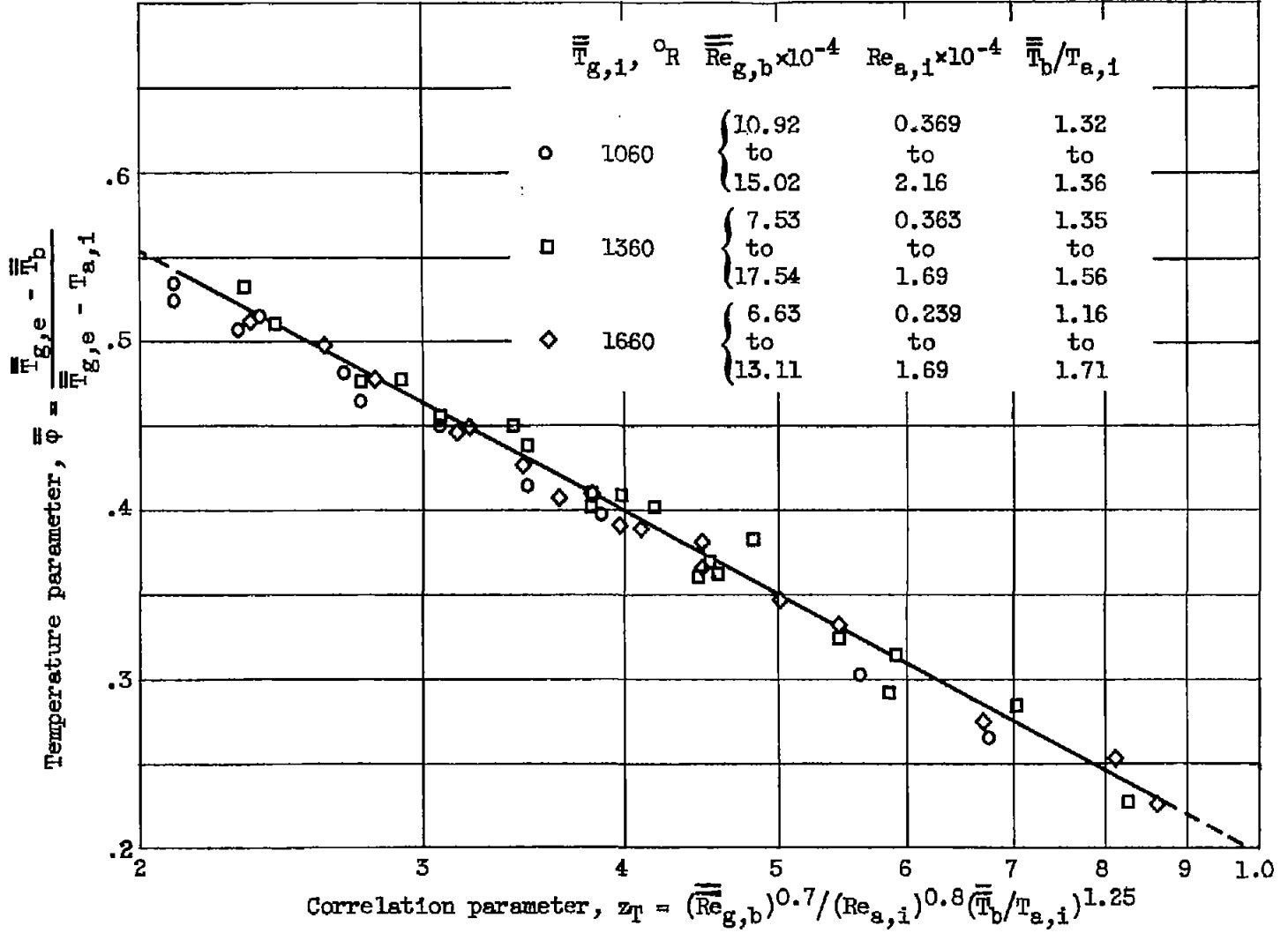


Figure 6. - Correlation of average blade metal temperatures.

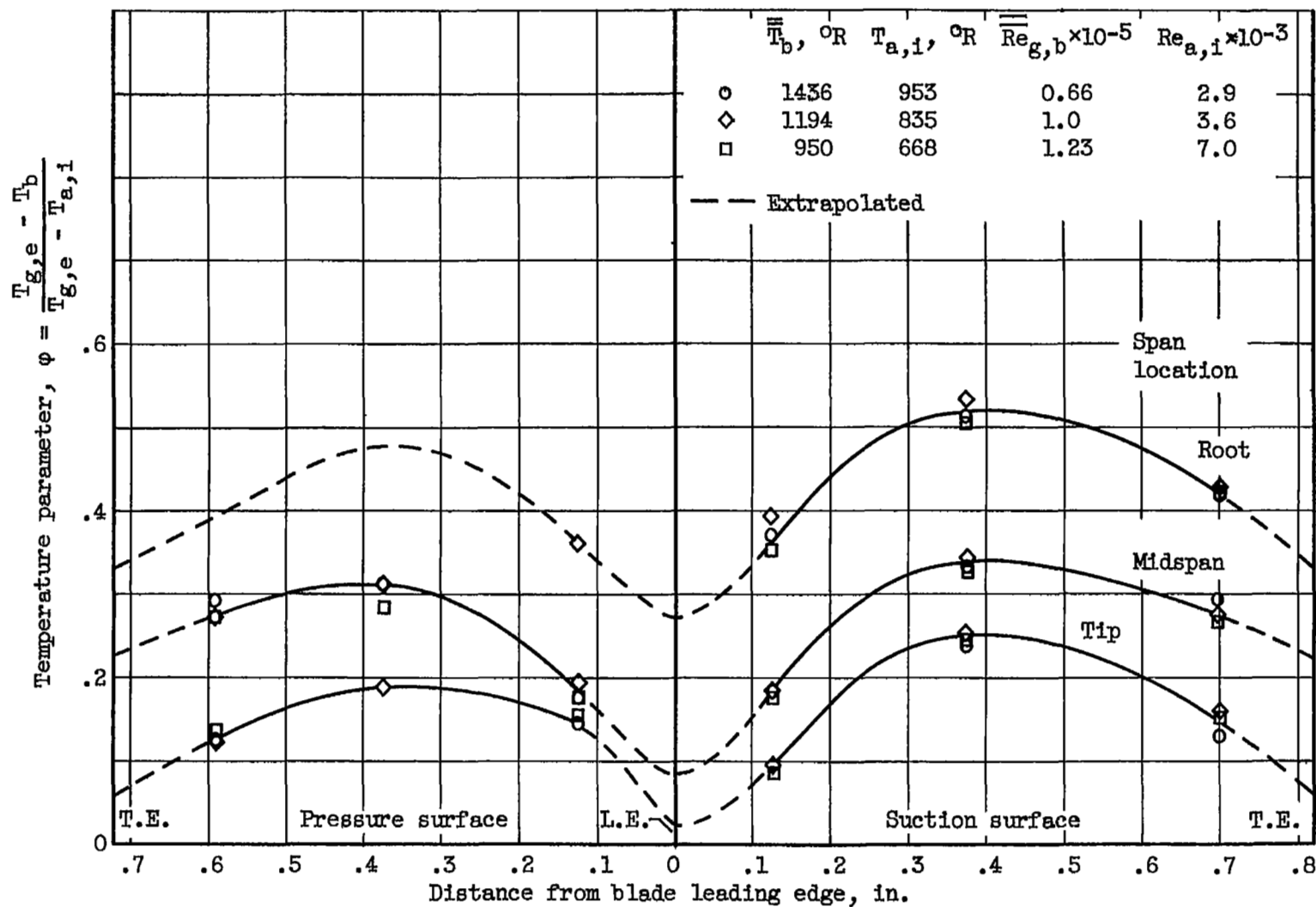


Figure 7. - Typical chordwise variations of local temperature parameter at three spanwise locations. (Data plotted for constant value of z_T of approx. 6.9.)

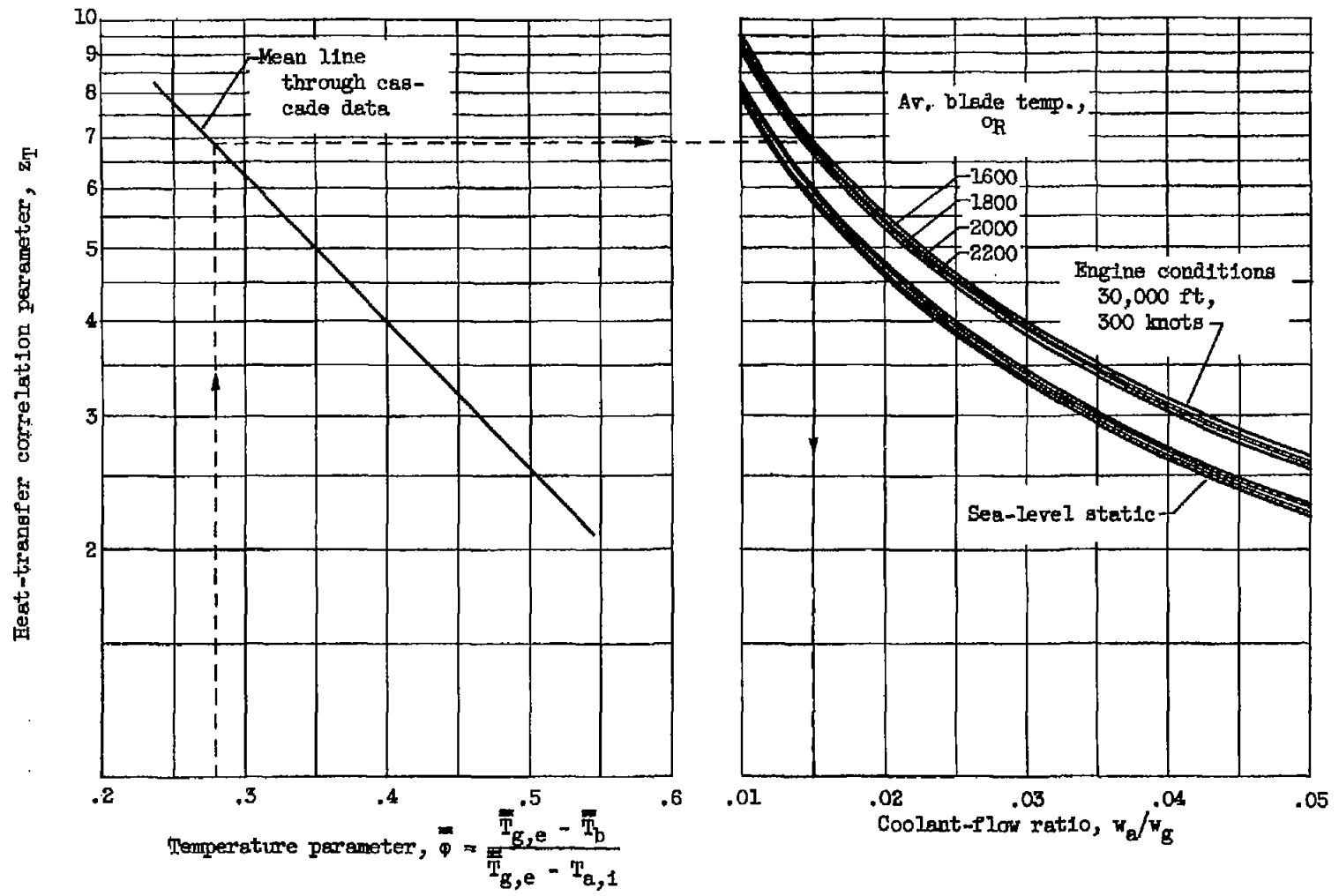


Figure 8. - Working chart for determining required coolant-flow ratio and desired cooled-blade temperature using correlation obtained from cascade tests.

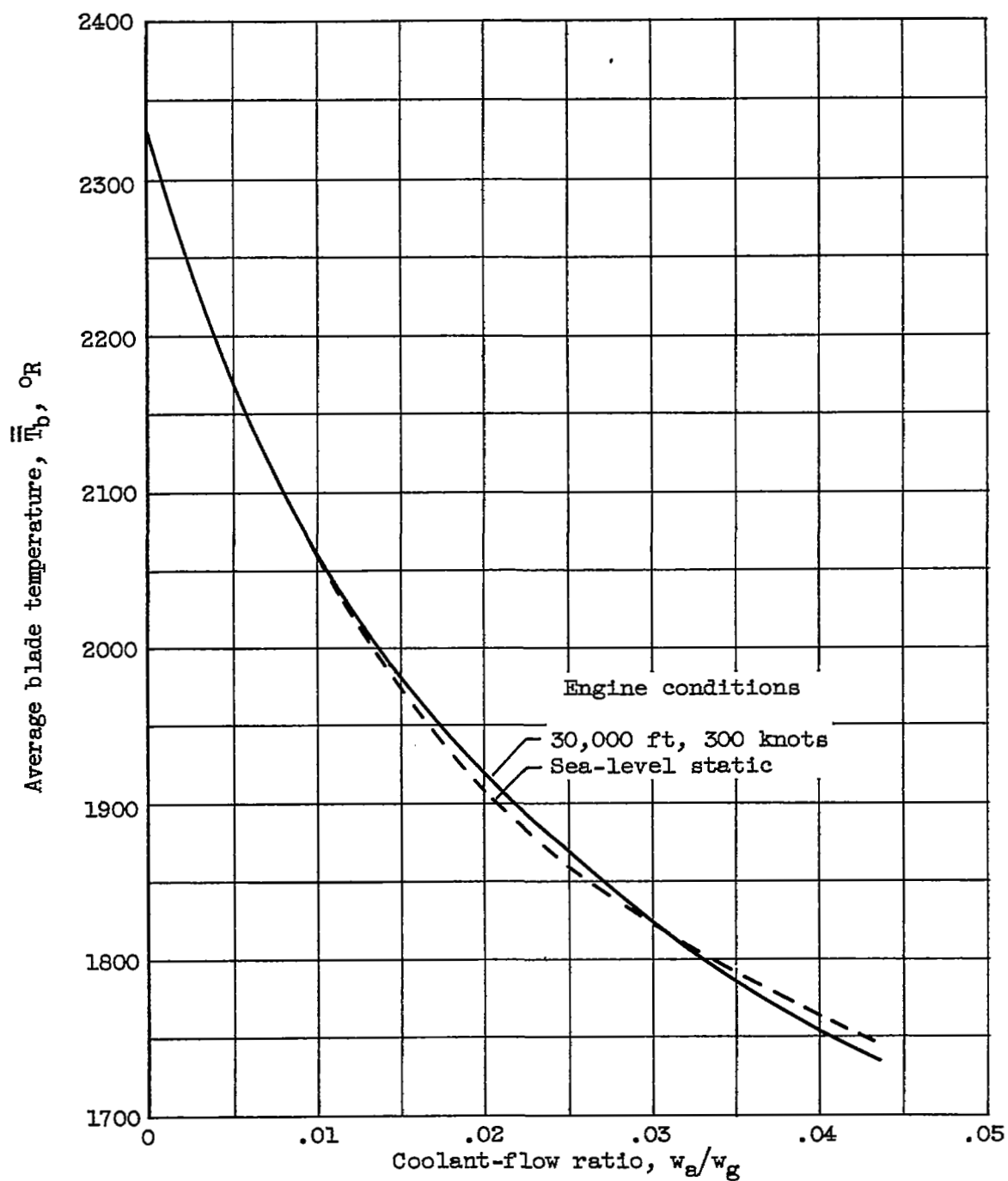


Figure 9. - Variation of calculated average blade temperature at turbine-inlet gas temperature of 2460° R with coolant-flow ratio.

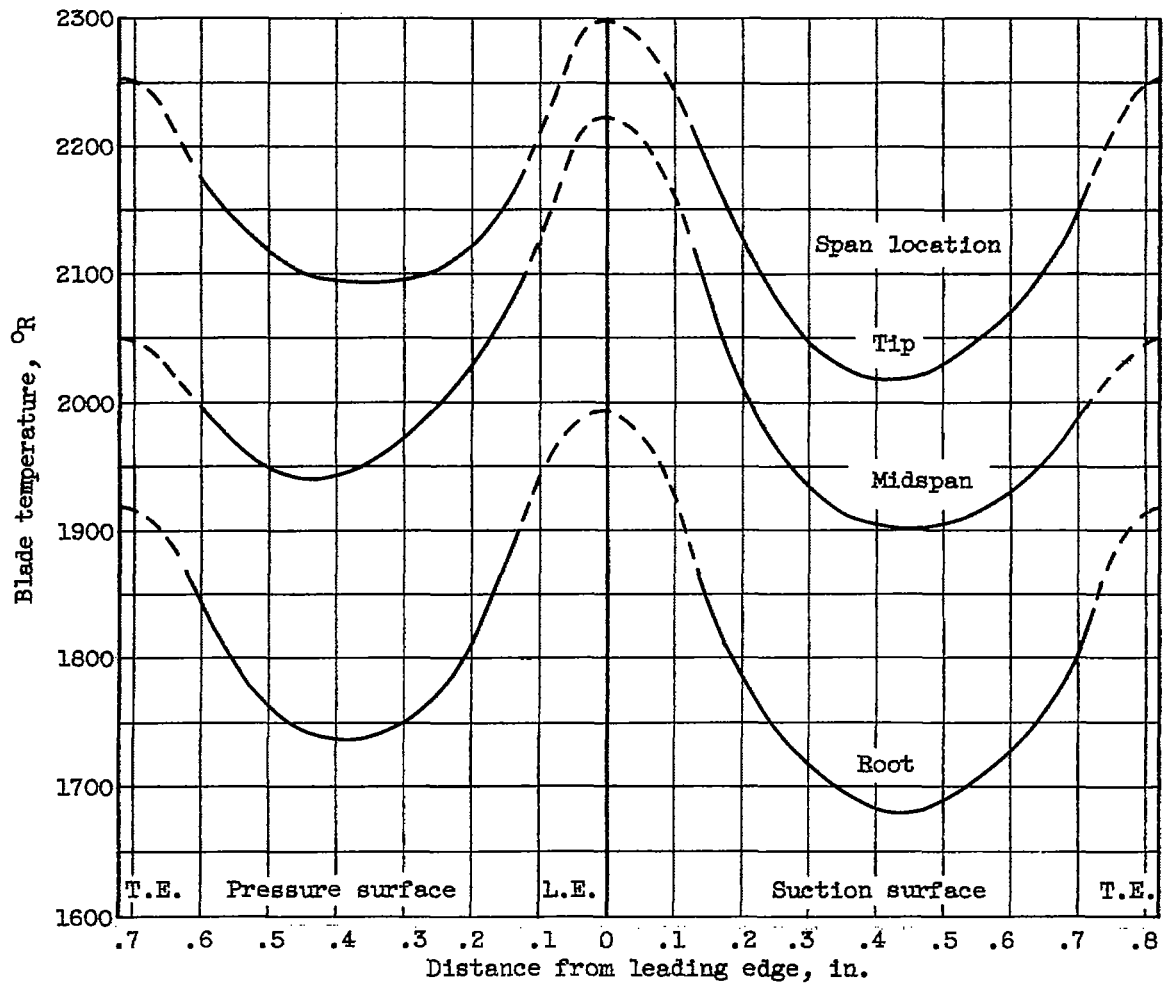


Figure 10. - Blade temperature distribution at turbine-inlet gas temperature of 2460° R, airspeed of 300 knots, altitude of 30,000 feet, and coolant-flow ratio of 0.015.

NASA Technical Library



3 1176 01436 5853

